

UvA-DARE (Digital Academic Repository)

Using Aliphatic Alcohols to Tune Benzene Adsorption in MAF-6

Martin-Calvo, A.; Gutierrez-Sevillano, J.J.; Dubbeldam, D.; Calero, S.

DOI

[10.1002/adts.201900112](https://doi.org/10.1002/adts.201900112)

Publication date

2019

Document Version

Final published version

Published in

Advanced Theory and Simulations

License

Article 25fa Dutch Copyright Act

[Link to publication](#)

Citation for published version (APA):

Martin-Calvo, A., Gutierrez-Sevillano, J. J., Dubbeldam, D., & Calero, S. (2019). Using Aliphatic Alcohols to Tune Benzene Adsorption in MAF-6. *Advanced Theory and Simulations*, 2(11), [1900112]. <https://doi.org/10.1002/adts.201900112>

General rights

It is not permitted to download or to forward/distribute the text or part of it without the consent of the author(s) and/or copyright holder(s), other than for strictly personal, individual use, unless the work is under an open content license (like Creative Commons).

Disclaimer/Complaints regulations

If you believe that digital publication of certain material infringes any of your rights or (privacy) interests, please let the Library know, stating your reasons. In case of a legitimate complaint, the Library will make the material inaccessible and/or remove it from the website. Please Ask the Library: <https://uba.uva.nl/en/contact>, or a letter to: Library of the University of Amsterdam, Secretariat, Singel 425, 1012 WP Amsterdam, The Netherlands. You will be contacted as soon as possible.

Using Aliphatic Alcohols to Tune Benzene Adsorption in MAF-6

Ana Martin-Calvo, Juan Jose Gutierrez-Sevillano, David Dubbeldam, and Sofia Calero*

This simulation study deals with benzene adsorption in the metal azolate framework, MAF-6, and on the inversion of the adsorption behavior in presence of aliphatic alcohols with varying chain length. To this aim, a new set of Lennard-Jones interacting parameters for the MAF structure with benzene, methanol, ethanol, and 1-propanol is developed in order to reproduce experimental adsorption. Pure component and binary benzene/alcohol mixtures are analyzed using Monte Carlo simulations. The distribution of the molecules inside the structure is studied in terms of radial distribution functions, calculated to understand the adsorption mechanisms. Adsorption selectivity provides a better understanding of the effect exerted by the adsorption of alcohols. It is found that the adsorption of benzene from benzene/methanol mixtures is similar to its pure component isotherm. However, for increasing length of the aliphatic chain of the alcohols the adsorption behavior is reversed preventing benzene to be adsorbed. The effect of open metal sites is discarded as main responsible for the preferential adsorption of alcohols, while the entropy and the molecular packing of alcohols are revealed as the reason for the different adsorption behavior of benzene.

1. Introduction

Benzene is a natural constituent of crude oil and it is also the most representative component from gasoline.^[1] However, restrictions imposed to gasoline in order to enhance fuels quality, force to reduce the benzene content decreasing the impact on human health and environment.^[2,3] Besides gasoline, benzene is one of the most common aromatic petrochemicals in the chemical industry, with diverse applications and a large commercial value. Among its uses, benzene plays an important role as solvent in paints or as intermediate chemical

product in the manufacture of plastics, drugs, dyes, detergents, and insecticides. About 55% of produced benzene is converted to ethylbenzene and used as an intermediate product on the production of synthetic rubber or plastic materials.^[4] On the other hand, benzene has been extensively used as entrainer on azeotropic distillation processes to break alcohol/water azeotropes. The separation of alcohol/water, benzene/water, and benzene/alcohols mixtures resulting from this particular process is still challenging.


Nevertheless, the carcinogenic nature of benzene limits its use and increases the interest of its removal. Therefore, adsorption and capture of benzene have been widely studied. Most studies deal with adsorption of benzene on transition metals surfaces,^[5,6] graphene,^[4,7,8] carbon nanotubes,^[9–11] activated carbons,^[12–14] zeolites,^[15–17] MOFs,^[18–20] or mesoporous materials.^[21–23] However, a recently developed material, MAF-6, appears as a promising candidate for the capture of

benzene from industrial processes.^[24] This metal azolate framework (MAF) is a large-pore metal-organic zeolite with an exceptional hydrophobicity. This property confers to the material special capabilities for oil/water separation, organic-pollutant enrichment, or chromatography analysis, among others.

To the best of our knowledge, most studies on MAF-6 deal with water adsorption^[25] and the separation of mixtures with industrial relevance such as 1-butanol from ABE fermentation broth,^[26] n-alkanes,^[27] or spilled oil^[28] and phthalic acid^[29] from water as cleaning contaminated water agent. Some studies use the structure of MAF-6 as template and carbon precursor of porous carbons applied for the removal of aromatic hydrocarbons, sweeteners, pharmaceutical, and personal care products from water.^[30–34] The most recent study on this material, shows a phase transition of the structure due to a combination of high pressure and non-wetting liquids during intrusion-extrusion experiments.^[35] We could not find reported studies exploring the adsorption mechanism of benzene in MAF-6 or its performance on the capture/separation of benzene/alcohol mixtures. The aim of this work is to fill this gap by studying at a molecular level the interactions between MAF-6 and benzene and to figure out the effect that aliphatic alcohols exert on benzene adsorption.

Dr. A. Martin-Calvo, Dr. J. J. Gutierrez-Sevillano, Prof. S. Calero
Department of Physical
Chemical and Natural Systems
University Pablo de Olavide
Sevilla 41013, Spain
E-mail: scalero@upo.es

Dr. D. Dubbeldam
Van't Hoff Institute for Molecular Sciences
University of Amsterdam
Amsterdam 1090 GD, The Netherlands

 The ORCID identification number(s) for the author(s) of this article can be found under <https://doi.org/10.1002/adts.201900112>

DOI: 10.1002/adts.201900112

2. Simulation Details

Molecular simulations are performed using the software package RASPA.^[36,37] Adsorption isotherms are computed using Grand Canonical Monte Carlo simulations, where the number of adsorbed molecules is obtained for a given chemical potential, volume, and temperature. The chemical potential is converted to pressure using the Peng–Robinson equation and the fugacity coefficient. To reach equilibrium, the molecules are allowed to move by using random moves: rotations, translation, regrow, insertion/deletion, and identity change (for mixtures). The acceptance probability of these moves is determined by the Boltzmann factor as described by Dubbeldam et al.^[37] It is important to note that these simulations, especially for alcohols, need to be long enough to ensure internal equilibrium (at least 10^6 equilibration and $2 \cdot 10^7$ production steps). To validate the interaction parameters, we compare the pure component isotherms resulting from simulation with experimental data. Experiments measure the difference between the amount of gas in the system and the amount that would be present at the same temperature and pressure in absence of adsorption (excess loading). Simulations calculate the total amount of molecules that could fit within the pores of the structure (absolute adsorption). To compare our simulated results with experimental values, the absolute loading needs to be converted to excess adsorption.^[38] To quantify the strength of the gas-structure interaction, heats of adsorption, and Henry coefficients are calculated with MC simulations in the NVT ensemble and using the Widom test-particle method.^[39]

Interactions within the system are defined by Lennard–Jones (L–J) and Coulombic potentials. Lorentz–Berthelot mixing rules are applied to guest–guest L–J interactions, while host–guest interactions are defined independently. A new set of L–J parameters between the structure with benzene and alcohols is provided in this work. To calculate the Coulombic interactions, we use the Ewald summation method with a relative precision of 10^{-6} . A *cutoff* of 12 Å is set. This is the distance at which the L–J and Coulombic potentials are cut and shifted.

Benzene is defined as a full atom rigid model where carbon and hydrogen atoms are considered as single Lennard–Jones interaction centers with point charges.^[40] Methanol, ethanol, and 1-propanol are modeled using TraPPE.^[41] This model defines CH_x groups as single interaction centers. The hydrogen and oxygen atoms of the hydroxyl group are defined independently. CH_x groups and OH atoms have Lennard–Jones and point charges applied, except for hydrogen atoms (from OH) that only have point charges assigned.

MAF-6 is modeled as a rigid framework, using the crystallographic position of the atoms.^[42] Lennard–Jones and point charges are applied to all atoms of the structure. L–J parameters are taken from DREIDING^[43] except for the metal atoms which are taken from UFF.^[44] Point charges are obtained from a transferable set of charges developed for Zeolitic Imidazolate Frameworks (ZIFs), multiplying these of the 2-ethylimidazole (eim) linker by a factor of 1.3.^[45] Force field parameters for the structure and the adsorbates are collected in **Table 1**, and the specific interactions developed in this work can be found in **Table 2**.

The structure of MAF-6 contains Zn metal atoms connected by 2-ethylimidazole linkers. This structure has big cavities of about 18 Å, communicated to each other forming a 3D network. A view

Table 1. Lennard–Jones parameters and point charges of the molecules and the structure.

Molecules			
Atom	ϵ [K/k_B]	σ [Å]	Charge [e^-]
C _{benz}	30.7	3.6	−0.095
H _{benz}	25.45	2.36	0.095
C H ₃ metOH	98	3.75	0.265
C H ₃ etOH	98	3.75	−
C H ₂ etOH	46	3.95	0.265
C H ₃ 1propOH	98	3.75	−
C H _{2a} 1propOH	46	3.95	−
C H _{2b} 1propOH	46	3.95	0.265
O _{OH}	93	2.9596	−0.7
H _{OH}	−	−	0.437
Structure			
Atom	ϵ [K/k_B]	σ [Å]	Charge [e^-]
N	38.95	3.26	−0.7683
Zn	62.4	2.46	2.6
C ₁	47.86	3.47	−0.1872
C ₂	47.86	3.47	0.3068
C ₃	47.86	3.47	−0.4654
C ₄	47.86	3.47	−0.6812
H ₁	7.65	2.85	0.1768
H ₃	7.65	2.85	0.2184
H ₄	7.65	2.85	0.2201

Table 2. Lennard–Jones parameters of the host–guest interactions.

Molecule-Structure			
Atom1	Atom2	ϵ [K/k_B]	σ [Å]
N	C _{benz}	48.411776	3.1899
N	H _{benz}	44.078384	2.6133
Zn	C _{benz}	61.275872	2.8179
Zn	H _{benz}	55.7910084	2.2413
C _{1/2/3/4}	C _{benz}	53.664072	3.28755
C _{1/2/3/4}	H _{benz}	48.860546	2.71095
H _{1/3/4}	C _{benz}	21.454972	2.99925
H _{1/3/4}	H _{benz}	19.534522	2.42265
N	C H ₃ OH	69.8144284	3.417375
Zn	C H ₃ OH	88.3657062	3.027375
C _{1/2/3/4}	C H ₃ OH	77.3887506	3.51975
H _{1/3/4}	C H ₃ OH	30.9401345	3.2175
N	C H ₂ OH	55.027	3.42475
Zn	C H ₂ OH	69.6489	3.04475
C _{1/2/3/4}	C H ₂ OH	60.997	3.5245
H _{1/3/4}	C H ₂ OH	24.3867	3.23
N	O _{OH}	68.0101348	3.0615
Zn	O _{OH}	61.275872	2.6715
C _{1/2/3/4}	O _{OH}	48.860546	2.71095
H _{1/3/4}	O _{OH}	21.454972	2.99925

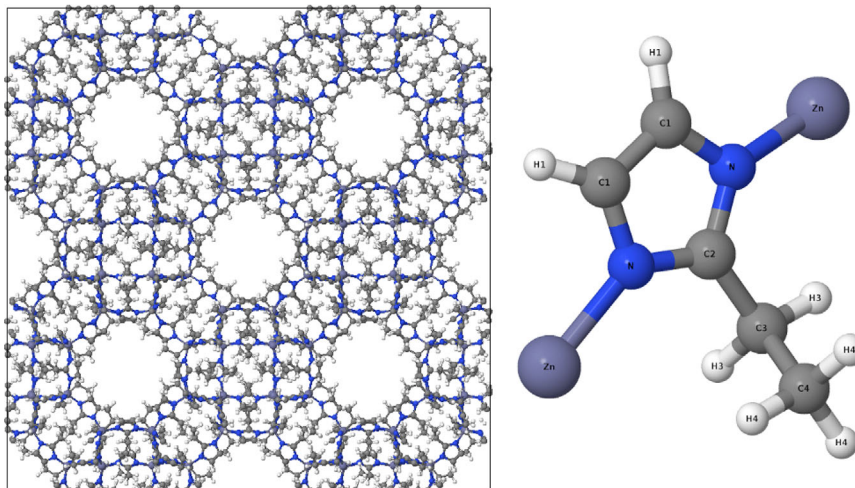


Figure 1. Schematic view of the structure^[42] (left) and description of the organic linker. Zn, N, C, and H atoms are represented in indigo, blue, grey, and white, respectively.

Table 3. Experimental and calculated Pore Size Distribution (PSD), Pore Volume (PV), and Surface Area (SSA).

Property	Experimental	Calculated
PSD [Å]	18.1 and 7.6	17 and 7
PV [$\text{cm}^3 \text{g}^{-1}$]	0.63	0.59
SSA [$\text{m}^2 \text{g}^{-1}$]	1695	1664

of the structure and a description of the organic linker with the atom labels used in this work are shown in **Figure 1**.

We analyze the structural properties of the material (**Table 3**). To this purpose, Pore Size Distribution (PSD), Pore Volume (PV), and Surface Area (SSA) are calculated and compared to experimental data.^[24] As observed from the table, small differences can be found between the pores of the experimental and the simulated materials. These differences are explained by the fact that the simulated structure^[42] is saturated with hydrogen while the experimental material^[24] (reported in the Cambridge Crystallographic Data Center as MECWOH) does not contain the H atoms from the ethyl groups. These small alterations are translated on slight PV and SSA deviations. However, differences are within reasonable errors.

3. Results and Discussion

Molecular simulation is a powerful tool to study static and dynamical properties of materials. However, the reliability of simulations depends on the models and force fields used. For this reason, the first step on simulation studies should be the force field validation. Generic mixing rules are commonly used to describe the interactions between the components of the system. Nonetheless, as shown for most zeolites and some MOFs, they do not always lead to accurate results.^[46] As in this work we use reported models for the adsorbates (TraPPE^[40,41]) and for the structure (Dreiding^[43] and UFF^[44]), we only need to check the accuracy

of the cross-interactions to reproduce experimental results, with Lorentz–Bertheloth mixing rules. **Figure 2**, shows the adsorption isotherms of benzene, methanol, ethanol, and 1-propanol at 298 K. The comparison with experimental data from the literature,^[24] shows the need of fitting the interaction parameters obtained by mixing rules. The figure shows that the isotherms obtained using mixing rules are shifted to higher values of pressure. This shift is larger for the longer alcohols, and specially remarkable for benzene, proving that mixing rules cannot be applied to this particular structure. Therefore, we defined specific values for the L–J parameters for the interactions of benzene and alcohols with the MAF-6 structure. With these new values, the saturation capacity is still slightly larger than in reported experiments, but the shape of the isotherms matches perfectly with the rise on adsorption at the same range of pressure. Focusing on the values of pressure at which the adsorption loading increases, we found similar values of pressure (about 10^2 Pa), for benzene and 1-propanol. The value of pressure increases for ethanol at 10^3 and methanol at $3 \cdot 10^3$ Pa. From these values we can deduce that the competition of benzene will be stronger with 1-propanol than with short alcohols.

Calculated isosteric heats of adsorption and Henry coefficients of the molecules at low coverage are shown in **Figure 3**. These properties provide molecular insights on the interaction of the molecules with the structure. Henry coefficients are related to the pressure at which the adsorbed molecules start entering the structure. As observed from the figure, Henry coefficients of methanol and ethanol are lower than these of 1-propanol, explaining the need of increasing pressure for the molecules to be adsorbed. On the other hand, 1-propanol and benzene show the highest Henry coefficients, confirming the previous statement on the competition between these two molecules. Based on the heats of adsorption, 1-propanol is the molecule with the strongest interaction with the MAF-6 structure, followed by ethanol, methanol, and finally by benzene. This is mainly due to the polarity of the alcohol molecules. The fact that the heat of adsorption increases with the length of the chain indicates that the shape and volume of the molecules are important too. A similar behavior was observed for alkanes up to C12 by Bhadra et al. on a previous

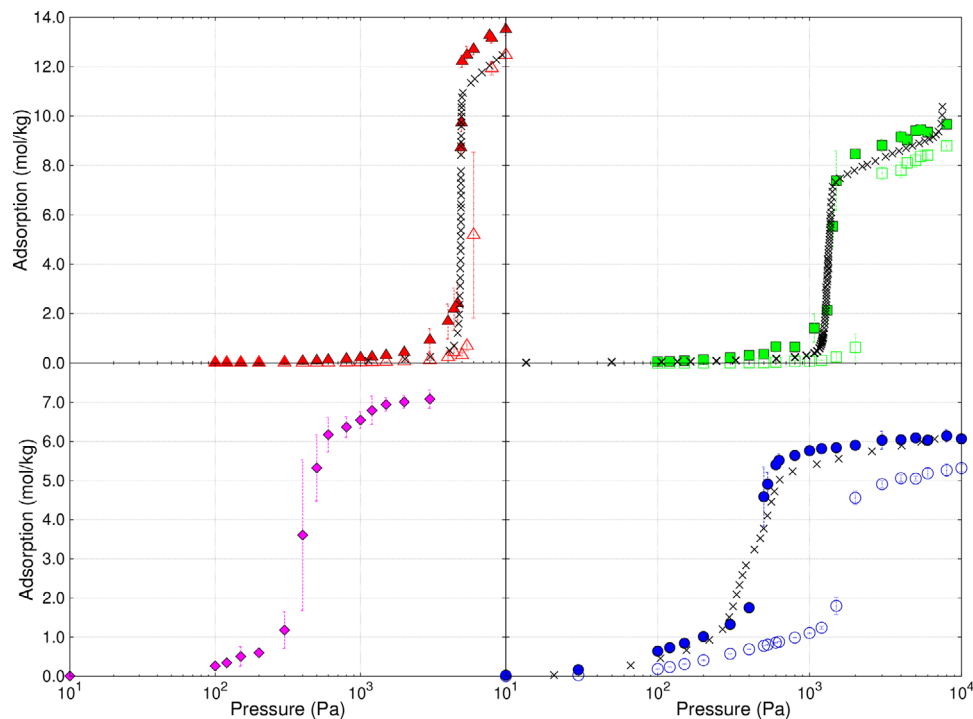


Figure 2. Adsorption isotherms of methanol (red triangles), ethanol (green squares), 1-propanol (pink diamonds), and benzene (blue circles) at 298 K. Comparison of experimental data^[24] (crosses), with calculated isotherms using generic mixing rules (empty symbols), and the new values for the cross-interactions parameters (full symbols).

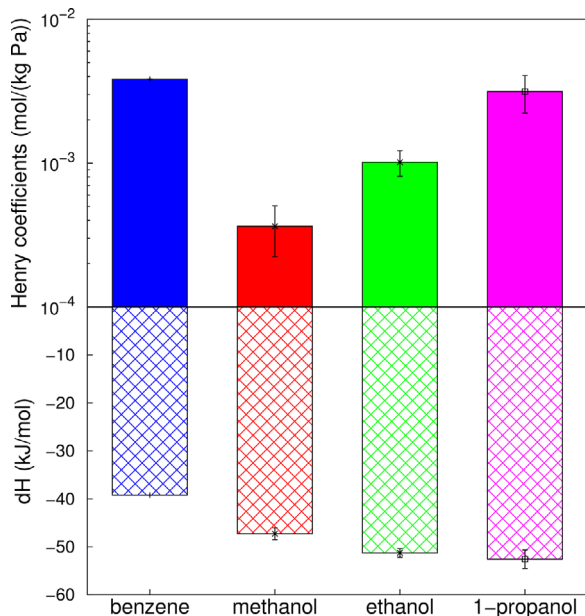


Figure 3. Heats of adsorption (crossed) and Henry coefficients (solid) of benzene (blue), methanol (red), ethanol (green), and 1-propanol (pink) in MAF-6 at 298 K.

work^[27]; however, different trends were found for MOFs other than MAF-6. The large difference between the heat of adsorption of benzene and 1-propanol confirms once more that 1-propanol is the molecule that will mostly interfere with benzene adsorption.

As observed, there is a clear relation between the heat of adsorption of alcohols and their chain length; therefore, we now evaluate the effect exerted by the chain length on the adsorption of benzene from the equimolar binary mixtures of benzene/methanol, benzene/ethanol, and benzene/1-propanol (Figure 4).

It is interesting to note that, up to 10^4 Pa, benzene adsorption from the benzene/methanol mixture is almost identical to its adsorption as pure component. The adsorption of methanol (below 1 mol kg^{-1}) is almost negligible compared to the adsorption of benzene. Although the interaction of methanol with the structure is stronger than the interaction benzene-structure, the latter is preferentially adsorbed. Benzene starts adsorbing at lower values of pressure than methanol, filling the structure and impeding the adsorption of methanol. Therefore, the stronger interaction of methanol with the atoms of the MAF is not enough to compete with the molecules of benzene. Above 10^4 Pa excess adsorption of benzene and methanol cannot be computed, therefore, only absolute adsorption values can be used, showing an inversion on the adsorption behavior in favor of methanol over benzene. Benzene adsorption at low and medium pressure is modified by alcohol molecules with more than one carbon atom. In the mixture with ethanol, the adsorption of benzene is about 1 mol kg^{-1} lower at saturation than in the mixture with methanol. Though, the adsorption of benzene is higher than the adsorption of ethanol, the isotherms exhibit similar trends up to 10^3 Pa. It is precisely at this value of pressure when the adsorption of benzene decreases compared to the pure and benzene/methanol isotherms. The adsorption of ethanol increases with pressure up to 3 mol kg^{-1} at $8 \cdot 10^3$ Pa. From this value of pressure only

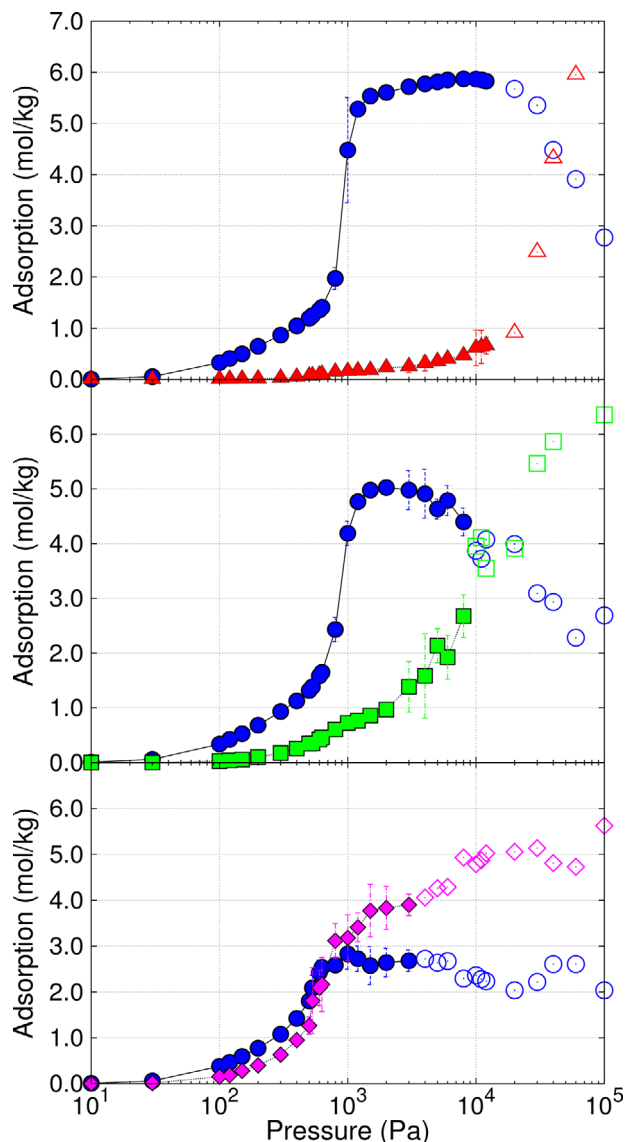


Figure 4. Equimolar binary mixtures of benzene (blue circles) with methanol (red triangles), ethanol (green squares), and 1-propanol (pink diamonds) at 298 K. Full symbols correspond to excess adsorption while empty symbols are used for absolute adsorption.

absolute adsorption data are shown. The trend of the adsorption isotherms at the highest values of pressure indicates that the adsorption could be larger for ethanol than for benzene. The adsorption isotherms of the mixture formed by benzene and 1-propanol show similar adsorption of the two components at low and medium values of pressure. The two gases start adsorbing at almost the same pressure and with similar strength. However, benzene reaches saturation at about 3 mol kg^{-1} while the adsorption of 1-propanol increases up to 4 mol kg^{-1} . At low loading, the competition of these two molecules can be explained by the combination of the higher heat of adsorption and lower Henry coefficient of 1-propanol compared to these of benzene (enthalpic effect), while at saturation pressure length and size entropies become important.^[47]

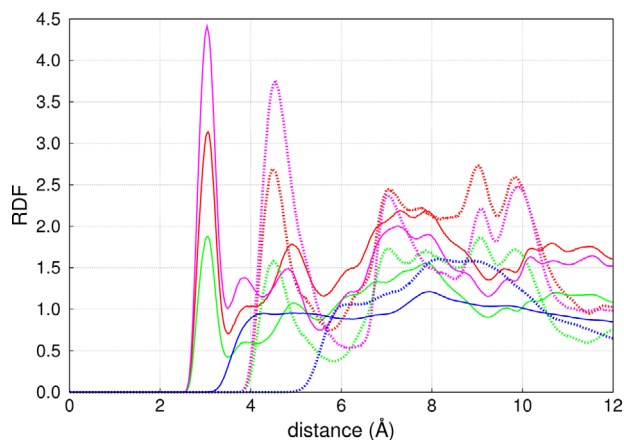


Figure 5. Radial Distribution Functions of the O atom from the hydroxyl group of the alcohols and the C₁ (solid lines) atoms of the framework. Methanol, ethanol, 1-propanol, and benzene are represented in red, green, pink, and blue, respectively. Data are taken from the pure component isotherms at the values of pressure at which the molecules start adsorbing in the structure (20, 24, 17, and 12 molec/u.c. of methanol, ethanol, 1-propanol, and benzene, respectively).

For a deepest understanding of the adsorption mechanism, we analyze the preferential position of the hydroxyl groups of the alcohols in the structure. As it happens with many metal-organic frameworks, the open metal sites in the structure could act as preferential adsorption sites for polar molecules, affecting therefore the adsorption of non-polar molecules as benzene. If this would be the case, the distance of the OH groups of the alcohol to the metal atoms of the structure (Zn) should be shorter than to any other atom of the structure. However, the Radial Distribution Functions (RDFs) of the oxygen atoms from the hydroxyl group to the atoms of the structure do not show this behavior. As shown in **Figure 5** the oxygen atoms of the hydroxyl groups are closed to the linker (C₁), discarding the open metal centres as preferential adsorption sites. The RDFs were calculated from the pure component isotherms at the values of pressure at which the molecules start adsorbing in the structure. Besides, we found similar peaks for the three alcohols with a peak at about 3 \AA from C₁ atoms against 4.5 \AA from Zn atoms. RDF between the Zn and C₁ atoms from the structure and the O atom from the hydroxyl group of alcohols obtained for pure components and mixtures with similar loading show identical peaks distribution. There is a lack of preferential adsorption sites for benzene in the structure at low loading. Nevertheless, as can be observed in **Figure 6** (left), for increasing pressure, benzene adsorbs closer to C₁ (peak at about 4 \AA). To determine if the presence of alcohols modifies this behavior, we computed RDFs in the mixtures at similar total loading (**Figure 6**, right). As shown, the adsorption of benzene close to C₁ is independent of the type of alcohol. We can conclude that the packing of benzene is due to the total density of molecules inside the structure.

The previous results indicate that the effect of the metal atoms is not responsible of the difference on benzene adsorption. Keeping in mind the competition between the molecules of benzene and the molecules of alcohols already discussed, we check if the packing of the alcohol molecules in the structure could be the

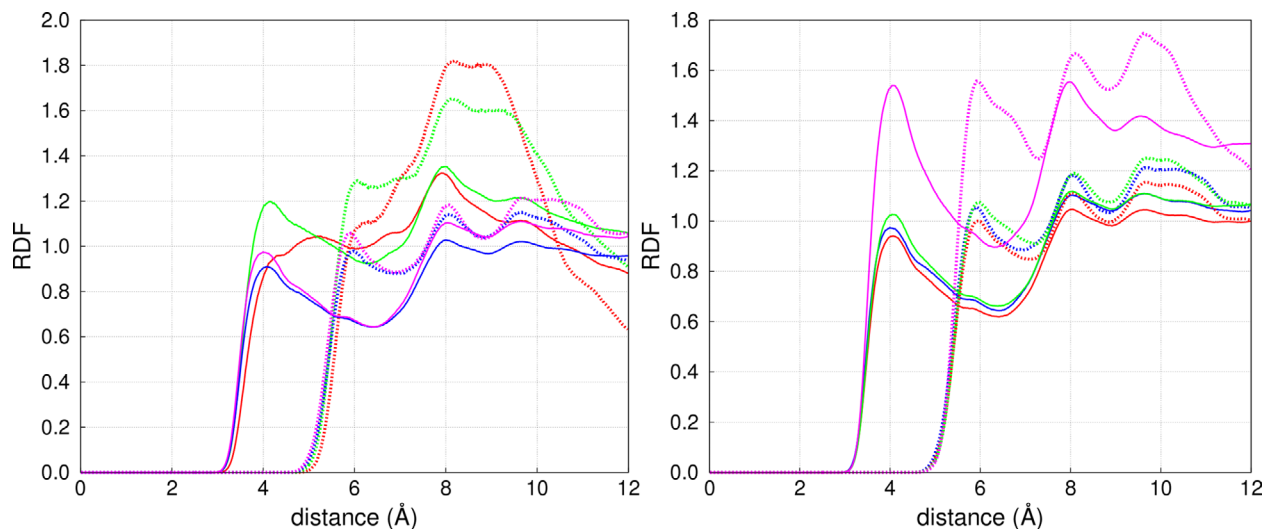


Figure 6. RDF of the C atom from benzene with the Zn (dotted lines) and the C_1 (solid lines) atoms of the framework from (left) the pure component isotherm as a function of pressure 100 Pa (red), 400 Pa (green), 500 Pa (blue), and 3000 Pa (pink) and (right) from the binary mixture with methanol (red), ethanol (green), and 1-propanol (pink), at similar total loading.

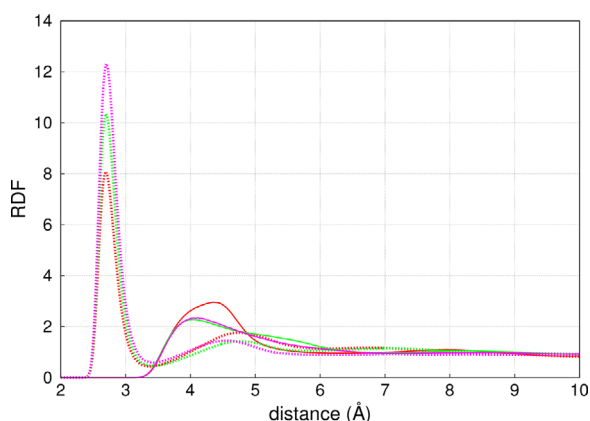


Figure 7. Radial Distribution Functions between the O atom from the hydroxyl groups (dotted line) and between the CH_3 group from the aliphatic chains (solid line) of methanol (red), ethanol (green), and 1-propanol (pink). Intra-molecular distances are excluded. Data are taken at saturation pressure.

reason of the variations on the loading of benzene. **Figure 7** shows the RDFs between oxygen atoms from the hydroxyl group and between the CH_3 groups from the aliphatic chain of the three alcohols under study at saturation pressure.

As seen in the figure, the distribution of OH groups is the same for the three alcohols and the peaks appear at about 2.6 Å. However, differences are observed at the end of the aliphatic chains, with larger distances between the CH_3 group of methanol (about 4.2 Å) than between the CH_3 group of ethanol and 1-propanol (at 3.9 Å, approx.). The fact that the distance is the same between hydroxyl groups but different between CH_3 groups indicates that the molecules of alcohol nucleate around the hydroxyl groups, probably due to the formation of hydrogen bonds. As shown in Figure 7, despite the larger chain of 1-propanol and ethanol compared to methanol, the peak of the latter appears at

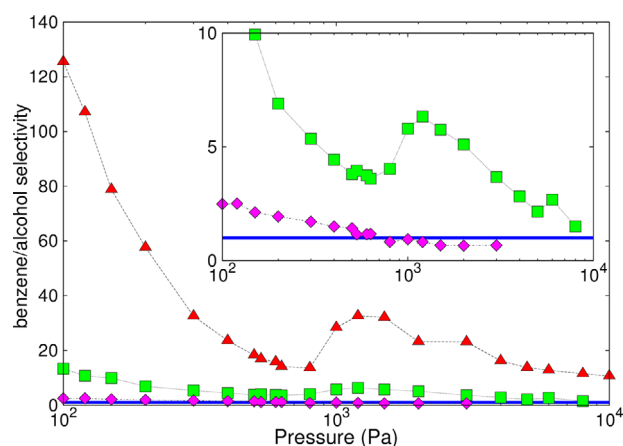


Figure 8. Adsorption selectivity of benzene over methanol (red triangles), ethanol (green squares), and 1-propanol (pink diamonds) at 298 K, calculated from the equimolar binary mixtures. Blue line at 1 indicates a lack of selectivity.

the longest distance. In other words, the packing of the molecules of methanol in the structure is worse than the packing of ethanol and 1-propanol molecules. Among the last two molecules (with almost identical peaks in the RDFs), the later packs better in the MAF-6 structure for being longer (length entropy). This better packing may favor its adsorption, hindering the adsorption of benzene.

The packing of the alcohols and the interactions of these molecules with the structure based on shape and size directly affect the adsorption of benzene. The influence can be also analyzed in terms of adsorption selectivity of benzene over the alcohol from the binary mixtures.

As shown in **Figure 8**, the selectivity of benzene over methanol is quite high, oscillating between 20 and 40. Note that as the adsorption of methanol at low pressure is almost zero, the

selectivity at this range of pressure seems high (larger than 100); however, this is nothing but an artifact. Besides, as the loading of methanol is low even at high pressure, any variation on the adsorption lead to large fluctuations on the selectivity. Between 10^3 and $5 \cdot 10^3$ Pa the selectivity is more or less constant (about 40), indicating that this structure preferentially adsorbs benzene. The selectivity of benzene over ethanol is much lower than over methanol. In this case the highest values of selectivity are around 10 and there is a change in the trend at 10^3 Pa, where the selectivity increases reaching values of about 6. At this value of pressure, the adsorption of ethanol increases smoothly while benzene reaches saturation. At $5 \cdot 10^3$ Pa the selectivity starts decreasing due to the rising adsorption of ethanol, thus preventing the adsorption of benzene from the structure. The selectivity of benzene over 1-propanol in MAF-6 is lower than 3 at low values of pressure. A twist on the selectivity can be seen above 10^3 Pa, with values below 1. This means that 1-propanol is preferably adsorbed over benzene, supporting the idea of tuning the adsorption of benzene by the addition of certain alcohols.

4. Conclusions

The effect of alcohols with increasing chain length (methanol, ethanol, and 1-propanol) on the adsorption of benzene in MAF-6 was evaluated using molecular simulations. The adsorption results of benzene in MAF-6 are similar as pure component than from equimolar binary mixture with methanol. However, this adsorption decreases when the mixture contains ethanol or 1-propanol instead of methanol. Contrary to the observed for other MOFs, there are not preferential adsorption sites for the polar molecules due to metal centers, and differences on benzene adsorption are due to size entropy, and in particular to the molecular packing of the alcohols (length entropy). The molecules of 1-propanol pack better than these of ethanol and methanol, and compete with benzene. Hence, the MAF-6 structure favors benzene over methanol and also over ethanol, but not over 1-propanol. Besides, at high pressure, the selectivity reverses in favor of 1-propanol. This fact might be used to modify ad hoc the adsorption and separation performance of benzene in MAF-6 by varying the alcohol of the adsorbed mixture.

Acknowledgements

This work was supported by the Spanish Ministerio de Ciencia, Innovación y Universidades (CTQ2016-80206-P) and the Ministerio de Ciencia, Innovación y Universidades (CTQ2017-92173-EXP and PCIN-2017-102). The authors thank C3UPO for the HPC support.

Conflict of Interest

The authors declare no conflict of interest.

Keywords

adsorption, alcohol, benzene, packing

Received: June 12, 2019
Revised: July 13, 2019
Published online: August 5, 2019

- [1] D. K. Verma, K. des Tombe, *AIHA J.* **2002**, *63*, 225.
- [2] M. A. Hanif, S. Nisar, U. Rashid, *Catal. Rev.* **2017**, *59*, 165.
- [3] S. R. Naqvi, A. Bibi, M. Naqvi, T. Noor, A. S. Nizami, M. Rehan, M. Ayoub, *Appl. Petrochem. Res.* **2018**, *8*, 131.
- [4] R. Nithyanandam, Y. K. Mun, T. S. Fong, T. C. Siew, O. S. Yee, N. Ismail, *J. Eng. Sci. Technol.* **2018**, *13*, 4290.
- [5] H. Yildirim, T. Greber, A. Kara, *J. Phys. Chem. C* **2013**, *117*, 20572.
- [6] W. Liu, J. Carrasco, B. Santra, A. Michaelides, M. Scheffler, A. Tkatchenko, *Phys. Rev. B* **2012**, *86*, 245405.
- [7] J. Björk, F. Hanke, C. A. Palma, P. Samori, M. Cecchini, M. Persson, *J. Phys. Chem. Lett.* **2010**, *1*, 3407.
- [8] D. Krepel, O. Hod, *J. Phys. Chem. C* **2013**, *117*, 19477.
- [9] F. Tournus, J. C. Charlier, *Phys. Rev. B* **2005**, *71*, 165421.
- [10] L. M. Woods, S. C. Bădescu, T. L. Reinecke, *Phys. Rev. B* **2007**, *75*, 155415.
- [11] F. Su, C. Lu, S. Hu, *Colloids Surf. A* **2010**, *353*, 83.
- [12] Y. C. Chiang, P. C. Huang, C. P. Huang, *Carbon* **2001**, *39*, 523.
- [13] M. A. Lillo-Rodenas, D. Cazorla-Amoros, A. Linares-Solano, *Carbon* **2005**, *43*, 1758.
- [14] J. W. Choi, N. C. Choi, S. J. Lee, D. J. Kim, *J. Colloid Interface Sci.* **2007**, *314*, 367.
- [15] C. J. Guo, O. Talu, D. T. Hayhurst, *AIChE J.* **1989**, *35*, 573.
- [16] S. Kasuriya, S. Namuangruk, P. Treesukul, M. Tirtowidjojo, J. Limtrakul, *J. Catal.* **2003**, *219*, 320.
- [17] N. Sivasankar, S. Vasudevan, *J. Phys. Chem. B* **2004**, *108*, 11585.
- [18] D. Britt, D. Tranchemontagne, O. M. Yaghi, *Proc. Natl. Acad. Sci. USA* **2008**, *105*, 11623.
- [19] Z. Zhao, S. Wang, Y. Yang, X. Li, J. Li, Z. Li, *Chem. Eng. J.* **2015**, *259*, 79.
- [20] W. Huang, J. Jiang, D. Wu, J. Xu, B. Xue, A. M. Kirillov, *Inorg. Chem.* **2015**, *54*, 10524.
- [21] C. Nguyen, C. G. Sonwane, S. K. Bhatia, D. D. Do, *Langmuir* **1998**, *14*, 4950.
- [22] M. Hartmann, C. Bischof, *J. Phys. Chem. B* **1999**, *103*, 6230.
- [23] M. Ghiaci, A. Abbaspur, R. Kia, F. Seyedeyn-Azad, *Sep. Purif. Technol.* **2004**, *40*, 217.
- [24] C. T. He, L. Jiang, Z. M. Ye, R. Krishna, Z. S. Zhong, P. Q. Liao, J. Xu, G. Ouyang, J. P. Zhang, X. M. Chen, *J. Am. Chem. Soc.* **2015**, *137*, 7217.
- [25] M. Gao, J. Wang, Z. Rong, Q. Shi, J. Dong, *RSC Adv.* **2018**, *8*, 39627.
- [26] C. Gao, Q. Shi, J. Dong, *CrystEngComm* **2016**, *18*, 3842.
- [27] B. N. Bhadra, S. H. Jhung, *ACS Appl. Mater. Interfaces* **2016**, *8*, 6770.
- [28] B. N. Bhadra, P. W. Seo, N. A. Khan, S. H. Jhung, *Inorg. Chem.* **2016**, *55*, 11362.
- [29] C. Wang, X. Yan, X. Hu, M. Zhou, Z. Ni, *J. Mol. Liq.* **2016**, *223*, 427.
- [30] S. Wang, T. Wang, P. Liu, Y. Shi, G. Liu, J. Li, *Mater. Res. Bull.* **2017**, *88*, 62.
- [31] X. W. Zhang, L. Jiang, Z. W. Mo, H. L. Zhou, P. Q. Liao, J. W. Ye, D. D. Zhou, J. P. Zhang, *J. Mater. Chem. A* **2017**, *5*, 24263.
- [32] B. N. Bhadra, J. Y. Song, S. K. Lee, Y. K. Hwang, S. H. Jhung, *J. Hazard. Mater.* **2018**, *344*, 1069.
- [33] J. Y. Song, B. N. Bhadra, N. A. Khan, S. H. Jhung, *Microporous Mesoporous Mater.* **2018**, *260*, 1.
- [34] H. J. An, B. N. Bhadra, N. A. Khan, S. H. Jhung, *Chem. Eng. J.* **2018**, *343*, 447.
- [35] B. Mortada, G. Chaplais, H. Nouali, C. Marichal, J. Patarin, *J. Phys. Chem. C* **2019**, *123*, 4319.
- [36] D. Dubbeldam, S. Calero, D. E. Ellis, R. Q. Snurr, *Mol. Simul.* **2016**, *42*, 81.

- [37] D. Dubbeldam, A. Torres-Knoop, K. S. Walton, *Mol. Simul.* **2013**, *39*, 1253.
- [38] T. Duren, R. Q. Snurr, *J. Phys. Chem. B* **2004**, *108*, 15703.
- [39] B. Widom, *J. Chem. Phys.* **1963**, *39*, 2808.
- [40] N. Rai, J. I. Siepmann, *J. Phys. Chem. B* **2007**, *111*, 10790.
- [41] B. Chen, J. J. Potoff, J. I. Siepmann, *J. Phys. Chem. B* **2001**, *105*, 3093.
- [42] X. C. Huang, Y. Y. Lin, J. P. Zhang, X. M. Chen, *Angew. Chem., Int. Ed.* **2006**, *45*, 1557.
- [43] S. L. Mayo, B. D. Olafson, W. A. Goddard, *J. Phys. Chem.* **1990**, *94*, 8897.
- [44] A. K. Rappe, C. J. Casewit, K. S. Colwell, W. A. Goddard, W. M. Skiff, *J. Am. Chem. Soc.* **1992**, *114*, 10024.
- [45] J. J. Gutierrez-Sevillano, S. Calero, C. O. Ania, J. B. Parra, F. Kapteijn, J. Gascon, S. Hamad, *J. Phys. Chem. C* **2013**, *117*, 466.
- [46] A. Martín-Calvo, F. D. Lahoz-Martín, S. Calero, *J. Phys. Chem. C* **2012**, *116*, 6655.
- [47] A. Torres-Knoop, D. Dubbeldam, *ChemPhysChem* **2015**, *16*, 2046.